

Differential Decoding for SFBC OFDM Systems in Underwater MIMO Channels

H. Eghbali*, Milica Stojanovic** and S. Muhaidat†

* Simon Fraser University, Burnaby, BC, Canada, V5A 1S6

** Northeastern University, Boston, MA 02115 USA

†University of Surrey, Guildford, United Kingdom

Email: * hea7@sfu.ca, ** militsa@ece.neu.edu, and † sami.muhammad@kustar.ac.ae

Abstract—We investigate the use of differential space frequency block codes (SFBCs) with orthogonal frequency division multiplexing (OFDM) over underwater acoustic channels. While SFBC efficiently exploits spatial transmit diversity, differentially coherent detection eliminates the need for extensive signal processing required for channel tracking. System performance is demonstrated using real data transmitted in the 12–26 kHz acoustic band from a vehicle moving at 0.5–2 m/s and received over a 100 m shallow water channel, using 4-QAM and a varying number of carriers ranging from 128 to 2048. Performance results demonstrate the advantage of the differentially coherent SFBC detection over the conventional, coherent SFBC detection which suffers from imperfect channel estimation.

I. INTRODUCTION

We consider orthogonal frequency division multiplexing (OFDM) for high-rate underwater acoustic (UWA) communications. By virtue of using a narrow-band signal on each of its multiple carriers, OFDM is easily conducive not only to multi-input-multi-output (MIMO) signal processing that exploits spatial diversity, but also to differentially coherent detection that eliminates the need for complex channel estimation [1], [2].

The feasibility of MIMO OFDM over UWA channels has been shown in recent experimental studies [3]–[6]. These systems have been considered for spatial multiplexing [3], [4], as well as for spatial diversity through Alamouti coding [5], [6]. In particular, while [5] considers Alamouti space-time block coding (STBC), [6] considers space-frequency block coding (SFBC). SFBC involves coding across OFDM carriers, whereas STBC involves coding across OFDM blocks in time. Due to the time-varying nature of the UWA channels, SFBCs are deemed better suited for use in these channels. Namely, STBCs require quasi static fades over adjacent OFDM blocks, which applies to slowly fading channels only. In contrast, SFBC require quasi static fades over adjacent OFDM carriers, which coincides with the basic OFDM design which calls for closely spaced carriers such that the channel frequency response can be considered as flat fading over each subband.

The use of Alamouti codes for gaining transmit diversity on UWA channels has been investigated exclusively within the framework of coherent detection, where major emphasis

is on developing accurate channel estimators. In contrast to coherent detection, differentially coherent detection does not require explicit channel estimation, and thus offers a solution that is computationally much simpler. Moreover, it can outperform the traditional coherent detection on highly time-varying channels, where channel estimation suffers from errors [2], [7].

In this paper, we consider differential SFBC as a means of obtaining transmit diversity over UWA channels without the need for explicit channel estimation. We apply differentially coherent detection to the experimental data obtained during the 2011 Kauai Acoustic Communications (KAM'11) experiment, where acoustic signals were transmitted over a 3 km long channel in the 20–32 kHz band. Comparison with coherent detection based on adaptive channel estimation [6] shows that differentially coherent detection can indeed be superior on a rapidly varying channel.

II. SYSTEM MODEL

We consider a MIMO OFDM system with $M_T = 2$ transmitters and M_R receivers. The system employs differential SFBC over K carriers, whose frequencies $f_k = f_0 + k\Delta f$, $k = 0, \dots, K - 1$, are separated by $\Delta f = B/K$, where f_0 is the lowest carrier frequency, and B is the system bandwidth. The information symbols belong to a QPSK alphabet, $b_k \in \{\pm \frac{1}{2} \pm j \frac{1}{2}\}$, $k = 0, \dots, K - 1$. These symbols are conveniently represented in a unitary matrix

$$\mathbf{B}_k = \begin{bmatrix} b_{2k} & -b_{2k+1}^* \\ b_{2k+1} & b_{2k}^* \end{bmatrix}. \quad (1)$$

Differential encoding is now applied, which yields a new unitary matrix of data symbols

$$\mathbf{D}_k = \mathbf{B}_k \mathbf{D}_{k-1}, \quad k = 1, \dots, K - 1. \quad (2)$$

The process starts with $\mathbf{D}_0 = \mathbf{B}_0$, and moves on across carriers. Although the elements of the differentially-encoded matrix-symbol \mathbf{D}_k belong to an expanded (non-PSK) constellation,¹ they obey the same symmetry rule as the elements of the original matrix-symbol \mathbf{B}_k , i.e.

$$\mathbf{D}_k = \begin{bmatrix} d_{2k} & -d_{2k+1}^* \\ d_{2k+1} & d_{2k}^* \end{bmatrix}. \quad (3)$$

¹ $d_k \in \{\pm \frac{1}{2} \pm j \frac{1}{2}, \pm 1, \pm j, 0\}$.

The differentially encoded symbols are finally used to modulate the OFDM carriers. SFBC is performed such that d_{2k} and d_{2k+1} are assigned to the carriers $2k$ and $2k+1$ of the first transmitter, while $-d_{2k+1}^*$ and d_{2k}^* are simultaneously assigned to the same carriers of the second transmitter.

Differential decoding is based on the fact that²

$$\mathbf{D}_k \mathbf{D}_{k-1}^H = \mathbf{B}_k, \quad (4)$$

which is also essential for differentially coherent detection.

The channel between the t^{th} transmitter and the r^{th} receiver is described by a set of complex-valued coefficients $H_k^{t,r}$ which represent the relevant channel transfer functions evaluated at frequencies f_k .

After FFT demodulation, the signals received on adjacent carriers of the r -th element are modeled as

$$\begin{aligned} y_{2k}^r &= H_{2k}^{1,r} d_{2k} + H_{2k}^{2,r} (-d_{2k+1}^*) + z_{2k}^r \\ y_{2k+1}^r &= H_{2k+1}^{1,r} d_{2k+1} + H_{2k+1}^{2,r} d_{2k}^* + z_{2k+1}^r, \end{aligned} \quad (5)$$

where z_k represents the noise, which is assumed to be circularly symmetric, zero-mean Gaussian, independent across carriers and receiving elements, and of equal power $E\{|z_k^r|^2\} = \sigma_z^2$.

The key assumption on which the Alamouti SFBC rests is that $H_{2k}^{t,r} \approx H_{2k+1}^{t,r}$. When this assumption holds, the received signal can be represented in a compact form. Specifically, if we define

$$\mathbf{Y}_k^r = \begin{bmatrix} y_{2k}^r & -y_{2k+1}^{r*} \\ y_{2k+1}^r & y_{2k}^r \end{bmatrix}, \mathbf{H}_k^r = \begin{bmatrix} H_{2k}^{1,r} & -H_{2k}^{2,r*} \\ H_{2k}^{2,r} & H_{2k}^{1,r*} \end{bmatrix}, \quad (6)$$

and make a similar matrix arrangement of the noise components, then (5) implies that

$$\mathbf{Y}_k^r = \mathbf{D}_k \mathbf{H}_k^r + \mathbf{Z}_k^r. \quad (7)$$

This matrix-signal easily lends itself to differentially coherent detection. Whereas a coherent detector would need to right-multiply \mathbf{Y}_k^r by a channel estimate $\hat{\mathbf{H}}_k^{rH}$, a differentially coherent detector simply multiplies it by \mathbf{Y}_{k-1}^{rH} , yielding

$$\mathbf{Y}_k^r \mathbf{Y}_{k-1}^{rH} = \mathbf{D}_k \mathbf{H}_k^r \mathbf{H}_{k-1}^{rH} \mathbf{D}_{k-1}^H + \text{noise terms}. \quad (8)$$

Differentially coherent detection now invokes a further assumption that $\mathbf{H}_k^r \approx \mathbf{H}_{k-1}^r$, i.e. coherence is required not only over two, but over four adjacent carriers. When that is the case, the inner channel matrix product reduces to a diagonal matrix

$$\mathbf{H}_k^r \mathbf{H}_{k-1}^{rH} = E_k^r \mathbf{I}, \quad (9)$$

where

$$E_k^r = |H_{2k}^{1,r}|^2 + |H_{2k}^{2,r}|^2 \quad (10)$$

is the total energy contained in the channels connecting the two transmitters with the r^{th} receiver (hence transmit diversity of order 2).

The remaining data symbols $\mathbf{D}_k \mathbf{D}_{k-1}^H$ conform to the decoding rule (4), and we thus have that

$$\mathbf{Y}_k^r \mathbf{Y}_{k-1}^{rH} \sim E_k^r \mathbf{B}_k + \text{noise terms}. \quad (11)$$

² H denotes conjugate transpose.

Casting the above observations into the multi-channel (receiver diversity) framework, we form the composite matrices

$$\begin{aligned} \mathbf{Y}_k &= [\mathbf{Y}_k^1 \dots \mathbf{Y}_k^{M_R}], \\ \mathbf{H}_k &= [\mathbf{H}_k^1 \dots \mathbf{H}_k^{M_R}], \end{aligned} \quad (12)$$

and express the received signal as

$$\mathbf{Y}_k = \mathbf{D}_k \mathbf{H}_k + \mathbf{Z}_k. \quad (13)$$

While pure maximum ratio combining (MRC) requires knowledge of the channel matrix \mathbf{H}_k , differential maximum ratio combining (D-MRC) relies on the variable

$$\mathbf{Y}_k \mathbf{Y}_{k-1}^H = \sum_{r=1}^{M+R} \mathbf{Y}_k^r \mathbf{Y}_{k-1}^{rH} \sim E_k \mathbf{B}_k + \text{noise terms}, \quad (14)$$

where

$$E_k = \sum_{r=1}^{M_R} E_k^r. \quad (15)$$

D-MRC thus yields the data symbol estimates

$$\hat{\mathbf{B}}_k = \frac{1}{\hat{E}_k} \mathbf{Y}_k \mathbf{Y}_{k-1}^H, \quad (16)$$

where \hat{E}_k can be calculated from the trace of $\mathbf{Y}_k \mathbf{Y}_k^H$. However, if the symbol estimates are directly used to make final decisions (i.e. no additional error correction coding is applied that would require soft-decision decoding), scaling by a positive value \hat{E}_k is irrelevant, and may be omitted.

The matrix $\mathbf{Y}_k \mathbf{Y}_{k-1}^H$ preserves the Alamouti structure, i.e.

$$\mathbf{Y}_k \mathbf{Y}_{k-1}^H = \mathbf{X}_k = \begin{bmatrix} x_{2k} & -x_{2k+1}^* \\ x_{2k+1} & x_{2k}^* \end{bmatrix}. \quad (17)$$

Hence, the original data symbols can be estimated from the first column of this matrix. The corresponding hard decisions are obtained as the nearest constellation points,

$$\begin{aligned} \tilde{b}_{2k} &= \text{dec}[\mathbf{Y}_k \mathbf{Y}_{k-1}^H]_{1,1}, \\ \tilde{b}_{2k+1} &= \text{dec}[\mathbf{Y}_k \mathbf{Y}_{k-1}^H]_{2,1}. \end{aligned} \quad (18)$$

III. EXPERIMENTAL RESULTS

The KAM'11 experiment was a multi-university research initiative focused on studying the impact of environmental fluctuations on underwater acoustic communication systems. The experiment was conducted off of the west coast of Kauai in a roughly 100 m deep water with downward refracting properties. Data were collected on a 16 element receiving array. Two independent sources, separated vertically by 15 m were used to transmit over approximately 3 km in the acoustic frequency range between 20 kHz and 32 kHz. The geometry of the experiment is shown in Fig. 1.

The bandwidth of the OFDM signal was $B = 12$ kHz, and the lowest carrier frequency was $f_0 = 20$ kHz. A zero-padded guard interval of duration $T_G = 60$ ms per OFDM block was used. The number of carriers used in the experiment varied from $K = 128$ to $K = 2048$. Each frame consisted of $N_d = 16384$ information symbols. For $K = 128, 256, 512, 1024, 2048$, each frame consisted of $N_b = 128, 64, 32, 16, 8$

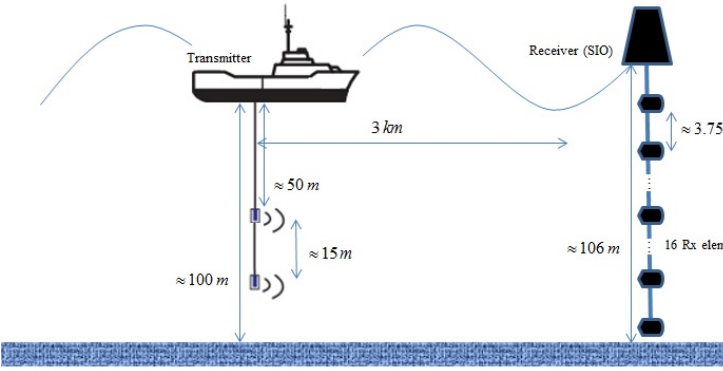


Fig. 1. Geometry of the KAM'11 experiment.

TABLE I
KAM'11 EXPERIMENT SIGNAL PARAMETERS

| | |
|-------------------------------------|--------------------------------|
| bandwidth, B [Hz] | 12000 |
| first carrier frequency, f_0 [Hz] | 20000 |
| sampling frequency, f_s [Hz] | 96000 |
| number of carriers, K | 128, 256, 512, 1024, 2048 |
| carrier spacing, Δf [Hz] | 93, 46, 23, 11, 5 |
| OFDM block duration, T [ms] | 10, 21, 43, 90, 200 |
| guard interval, T_G [ms] | 60 |
| symbols per frame, N_d | 16384 4-QAM |
| blocks per frame, N_b | 128, 64, 32, 16, 8 |
| bit rate, R [kbps] | 3.65, 6.32, 9.94, 13.65, 15.75 |

blocks, respectively. Table I summarizes the signal parameters used in the experiment.

After initial frame-synchronization and resampling (to compensate coarsely for the major Doppler scaling), the received signals were FFT-demodulated and passed on to differentially coherent detection and decoding. Fig. 2 shows the results obtained using 12 and 16 receiving elements. This figure shows the mean squared error (MSE) at the input to the decision device, as function of the number of carriers (log scale). Results are also provided for single-transmitter differential OFDM based on the method [7] and coherent SFBC OFDM based on the method [6]. Fig. 2 demonstrates that differential SFBC OFDM outperforms the single-transmitter differential OFDM, thus offering a spatial diversity gain. More importantly, it shows that differential SFBC indeed outperforms its coherent counterpart. As the number of carriers in the given bandwidth is increased, adaptive channel estimation becomes more difficult across longer blocks, causing coherent detection to fail with $K > 512$. In contrast, narrower carrier spacing enhances frequency coherence between adjacent carriers, allowing superior performance of differential SFBC with up to 2048 carriers (compared to 512 carriers, 2048 carriers provide a 78% increase in bit rate).

Fig. 3 illustrates the MSE performance of the differential SFBC OFDM receiver for a varying number of receiving elements. The performance is again shown in terms of the MSE at the input to the decision device. At least four receiving elements are needed in this system to provide a reliable performance with MSE consistently below -5 dB. Performance improves with the further increase in number of receiving elements, but we note an effect of diminishing returns.

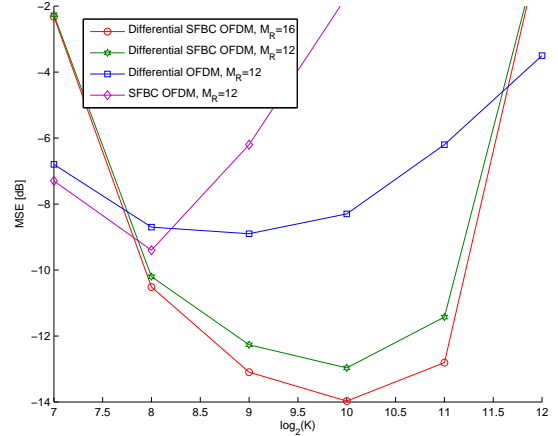


Fig. 2. Mean squared error (prior to symbol decision making) vs. the number of carriers.

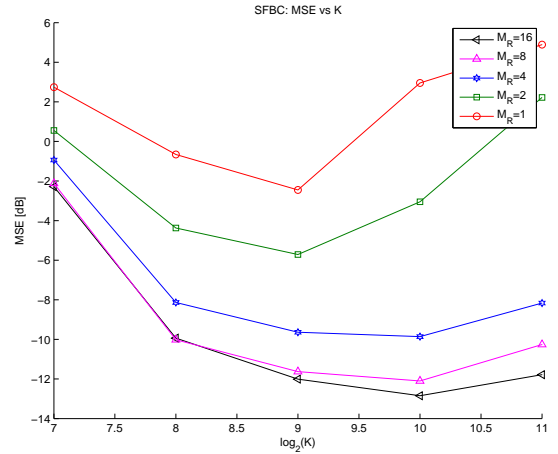


Fig. 3. MSE vs. the number of carriers for varying number of receiving elements.

Fig. 4 illustrates the corresponding symbol error rate (SER) performance. There is no additional error correction coding in this example. Nonetheless, multi-channel combining significantly improves the system performance, bringing the raw SER below $10e^{-3}$ with 10 or more receiving elements.

IV. CONCLUSION

We investigated differential SFBC as a means of gaining transmit diversity over underwater acoustic channels without the need for adaptive channel estimation. Compared with coherent detection, this approach is not only less demanding computationally, but offers an improvement in performance when time-variability challenges the accuracy of channel estimation. Our results demonstrated this fact using real data recorded over a shallow water channel within 12 kHz of acoustic bandwidth. Specifically, differential SFBC was shown to remain operational with up to 2048 carriers (16 kbps), while coherent SFBC failed with more than 512 carriers (10 kbps). Compared with the single-transmitter differentially coherent system, Alamouti SFBC scheme demonstrated an

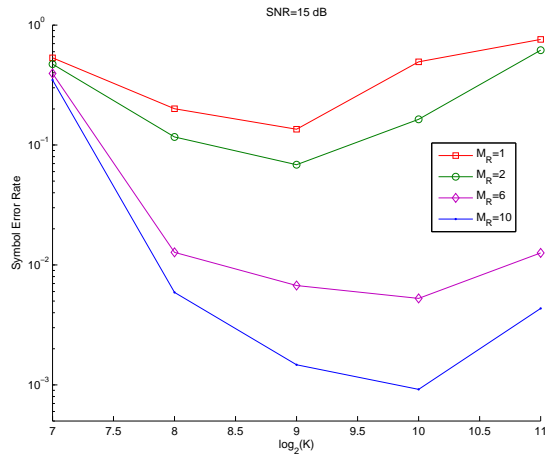


Fig. 4. SER vs. the number of carriers for different number of receiving elements.

improvement of about 6 dB in the mean squared detection error.

REFERENCES

- [1] H. Eghbali, and S. Muhaidat, "Precoded Differential OFDM for Relay Networks, *Journal of Selected Areas in Telecommunications*, p. 59-66, Jan. 2011.
- [2] S.Lu and N.Al-Dhahir, "Coherent and differential ICI cancellation for mobile OFDM with application to DVB-H," *IEEE Trans. Wireless Commun.*, vol. 11, no. 12, pp. 4110-4116, Nov. 2008
- [3] M. Stojanovic, "Mimo OFDM over underwater acoustic channels," in *Signals, Systems and Computers, 2009 Conference Record of the Forty Third Asilomar Conference on*, Nov. 2009, pp. 605-609.
- [4] B.Li, J.Huang, S.Zhou, K.Ball, M.Stojanovic, L.Freitag and P.Willett, "MIMO-OFDM for high rate underwater acoustic communications," *IEEE J. Oceanic Eng.*, vol. 34, no. 4, pp. 634-644, Oct. 2009.
- [5] B. Li and M. Stojanovic, "A simple design for joint channel estimation and data detection in an Alamouti OFDM system," in *OCEANS 2010*, Sept. 2010, pp. 1-5.
- [6] E. V. Zorita and M. Stojanovic, "Space-frequency block coding for underwater acoustic communications," *IEEE J. Oceanic Eng.*, to appear.
- [7] Y. Aval and M. Stojanovic, "A method for differentially coherent multi-channel processing of acoustic OFDM signals," in *7th IEEE Sensor Array and Multichann. Sig. Proc. Workshop (SAM)*, Jun. 2012.